Practical Considerations in the Design of Distribution State Estimation Techniques

Moosa Moghimi Haji, Omid Ardakanian
University of Alberta, Canada
{moghimih, oardakan}@ualberta.ca

***Abstract*—Distribution state estimation is crucial for planning and operation of active distribution networks. This paper extends two state-of-the-art state estimation techniques, namely Weighted Least Squares (WLS) and Ensemble Kalman Filter (EnKF), to unbalanced three-phase distribution networks. These networks are assumed to be equipped with smart meters and distribution-level phasor measurement units (D-PMUs), which are capable of measuring voltage and current phasors. We evaluate the two state estimation methods through extensive simulations in realistic settings where the secondary (low voltage) distribution system is accurately modelled, D-PMUs are installed only at a small number of buses in the primary system, and their measurements are noisy and become available for state estimation after a certain delay. Our results indicate that both methods achieve a sufficiently low error despite the small number of installed D-PMUs, and while EnKF outperforms WLS in some scenarios, the difference between the results gets smaller with more accurate D-PMU measurements. When both voltage and current phasor measurements are available, WLS yields more accurate results under realistic assumptions and is therefore more suitable for real-world applications.**

***Index Terms*—State estimation, power distribution system, phasor measurement unit, ensemble Kalman filter, weighted least squares.**

I. Introduction

The large-scale installation of renewable energy systems, such as solar photovoltaics and wind turbines has transformed the distribution system from a passive to an active network with bidirectional power and information flows, and complex dynamics that span multiple timescales. The expected growth in the adoption of electric vehicles, and proliferation of energy storage devices and power electronics will exacerbate the complexity of the network even further. This calls for a new control paradigm which requires accurate monitoring of the distribution system through various types of sensors along with distribution system estate estimation (DSSE) tools [1]–[3].

The weighted least square (WLS) method is traditionally used to solve the state estimation problem at the transmission level relying on redundant data from various sources [4]. But unlike transmission systems which are fully monitored, distribution systems contain a considerably larger number of components and are currently monitored only at a small number of locations across the network for cost reasons. Therefore, state estimation techniques that can deal with limited visibility and other specific requirements of distribution system, such as unbalanced loads and radial network configuration, must be developed [5]. In previous work, the WLS method has been extended to distribution system; this includes node voltage based methods [6] and branch current based methods [7]. The system states (i.e. node voltages or branch currents) are represented in either polar or rectangular form. A review of different WLS methods for DSSE can be found in [8].

If the measurement errors are independent, identically distributed and follow a Gaussian distribution, the WLS objective function gives the best possible performance except for specific ill-conditioned cases [9]. However, the limitation of WLS-based methods is that they solve the problem in a single snapshot and do not incorporate any information from the previous states. To address this shortcoming, several attempts have been made to date to utilize forecast-aided state estimation methods, such as Kalman filters, to improve over WLS [10], [11]. However, most of these methods failed to improve upon WLS-based methods. In recent work, Carquex et al. [12] proposed a method based on Ensemble Kalman Filter (EnKF) for DSSE and showed that it outperforms WLS. However, the two methods are only compared in a balanced 33-bus test system containing only the primary distribution nodes. Moreover, it is assumed that D-PMUs only capture voltage measurements and that they are available to the state estimator without any delay. These assumptions do not hold in practice. Thus, a more comprehensive comparison between WLS and EnKF-based methods is warranted to understand which method is more suitable for real-world implementation.

This paper seeks to provide a more comprehensive and realistic comparison between two state-of-the-art state estimation techniques which are reported to exhibit superior performance for DSSE. Our contribution is twofold:

- We extend the state-of-the-art state estimation techniques to make them suitable for performing real-time state estimation in unbalanced three-phase networks[1]. We explain how current phasors can be incorporated in the problem formulation to improve the state estimation accuracy.
- We carry out a thorough comparison between WLS and EnKF-based methods by studying how the number and precision of D-PMUs, communication delay, and time step of performing state estimation affect the results.

The rest of the paper is organized as follows: Section II describes the state estimation problem. The WLS and EnKF-based DSSE methods are briefly presented in Section III and evaluated through simulations carried out on a 33-bus system in Section IV. Section V concludes the paper and provides directions for future work.

[1]Our code is written in MATLAB and can be downloaded from GitHub: https://github.com/sustainable-computing/benchmarking-state-estimators

978-1-5386-8099-5/19/$31.00 ©2019 IEEE

II. State Estimation

State estimation (SE) is a process that concerns estimating the state(s) of a system utilizing redundant data from several sources, including measurements and pseudo-measurements. The state variables are usually voltage phasors of the nodes denoted by $x = [\theta_2, \theta_3, ..., \theta_N, v_1, v_2, ..., v_N]$, where N is the total number of nodes [8]. The phase angle of the first node is considered as the reference, hence it is not included in the state vector. We note that this vector uniquely determines the state of the power system because other unknown variables such as current phasors can be computed accordingly from the load flow equations. Other representations of the state, such as imaginary and real parts of the voltage, phase angle and magnitudes of the line currents, and real and imaginary parts of the line currents are equally valid and could be used for state estimation [13].

To solve the state estimation problem, we need to have three types of data [8]:

- **The network model** representing the network configuration and line parameters (impedance/admittance values). Although the network model is usually available for transmission systems, it may not be known for distribution systems in practice due to the lack of instrumentation beyond the distribution substation, frequent reconfiguration of feeders, and connection of new loads. Nevertheless, the network configuration and model parameters can be learned from the available measurements as discussed in [14]. In this paper we make the common assumption that the network model is available to the state estimator.
- **Real-time measurements** which could be acquired from the distribution supervisory control and data acquisition (DSCADA) and the distribution automation system, or collected by a network of D-PMUs. A D-PMU is a networked sensor which is specifically designed for distribution systems and can provide synchronized three-phase voltage and current phasors for a certain location in the distribution network. D-PMUs are not currently installed at a large number of buses due to cost reasons.
- **Load demands** which could be measured by end-devices such as smart meters or predicted based on historical data. Note that smart meters typically sample the load data every 15 minutes or longer, which is much slower than the sampling rate of D-PMUs. In addition, most of the commercial meters rolled out today merely report the sampled data at the end of the day [12]. Therefore, load demand data is unavailable in an online fashion for state estimation. To alleviate this problem, *pseudo-measurements*, which are load demand predictions based on historical load data, are used.

III. Methodology

In this section we briefly explain two powerful techniques, namely WLS [15] and EnKF [12], which have been applied to solving the distribution state estimation problem in the literature. A detailed description of these techniques can be found in the corresponding references.

A. Weighted Least Squares-based State Estimation

Figure 1 summarizes the state estimation process using the WLS method. The first step is to collect the required data which

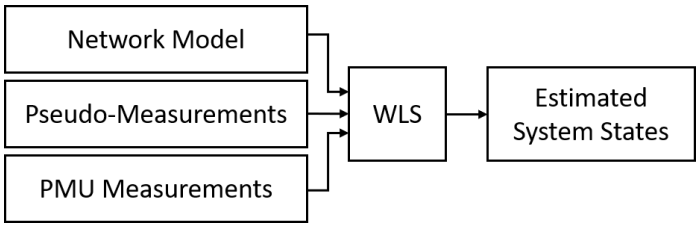

Fig. 1. An illustration of WLS-based state estimation process.

are: a) the network model encoded by the nodal admittance matrix, b) D-PMU measurements of voltage and current phasors, and c) pseudo-measurements which are the (predicted) real and reactive power consumption of the loads at the primary nodes. The covariance matrix of the measurement errors needs to be defined as discussed later.

Let us denote the measurement vector by z. We can write

$$z = h(x) + e, \tag{1}$$

where

$$z = \begin{bmatrix} z_1 \\ z_2 \\ \vdots \\ z_m \end{bmatrix}, h(x) = \begin{bmatrix} h_1(x_1, x_2, \cdots x_n) \\ h_2(x_1, x_2, \cdots x_n) \\ \vdots \\ h_m(x_1, x_2, \cdots x_n) \end{bmatrix}, e = \begin{bmatrix} e_1 \\ e_2 \\ \vdots \\ e_m \end{bmatrix},$$

x is the system state vector, $h_i(x)$ is a nonlinear function that relates the state vector to the ith measured value, and e is a vector that collects measurement errors. The errors are assumed to be independent random variables with zero mean and finite variance. This results in a diagonal covariance matrix $R = \text{diag}\{\sigma_1^2, \sigma_2^2, ..., \sigma_m^2\}$.

The basic idea of WLS is to determine the system states that minimize the difference between the measurement values and the corresponding values from the measurement function. To this end, the WLS-based method minimizes the following objective function [15]:

$$J(x) = [z - h(x)]^\top R^{-1}[z - h(x)]. \tag{2}$$

Note that the inverse of the error covariance matrix is multiplied in the above equation to give higher weights to more accurate measurements and diminish the effect of inaccurate measurements. Computing the solution requires the measurement function and its Jacobian. In our work, three-phase line current phasors are also considered. To derive the measurement function for line currents, we consider an unbalanced three-phase line for which the current flowing from the sending node to the receiving node is given by:

$$\vec{I}_{3ph} = \begin{bmatrix} \vec{I}_a \\ \vec{I}_b \\ \vec{I}_c \end{bmatrix} = \begin{bmatrix} y_{11} & y_{12} & y_{13} \\ y_{21} & y_{22} & y_{23} \\ y_{31} & y_{32} & y_{33} \end{bmatrix} \times \begin{bmatrix} \vec{V}_{a1} - \vec{V}_{a2} \\ \vec{V}_{b1} - \vec{V}_{b2} \\ \vec{V}_{c1} - \vec{V}_{c2} \end{bmatrix} \tag{3}$$

We can separate the real and imaginary parts of the equations to simplify deriving the Jacobian function. For example, the real

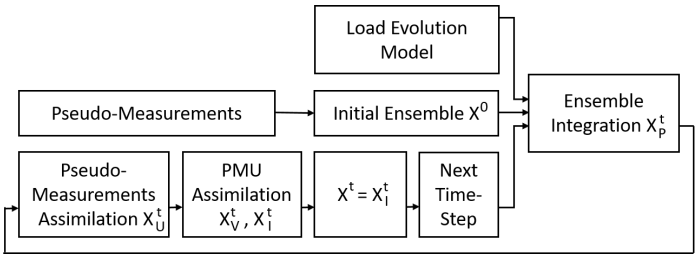

Fig. 2. An illustration of EnKF-based state estimation process.

and imaginary parts of Phase A current are:

$$
\begin{aligned}
&I_{a,real} = \\
&g_{11}(V_{a1}cos\theta_{a1}-V_{a2}cos\theta_{a2})-b_{11}(V_{a1}sin\theta_{a1}-V_{a2}sin\theta_{a2})+\\
&g_{12}(V_{b1}cos\theta_{b1}-V_{b2}cos\theta_{b2})-b_{12}(V_{b1}sin\theta_{b1}-V_{b2}sin\theta_{b2})+\\
&g_{13}(V_{c1}cos\theta_{c1}-V_{c2}cos\theta_{c2})-b_{13}(V_{c1}sin\theta_{c1}-V_{c2}sin\theta_{c2}), \quad (4)\\
&I_{a,imag} = \\
&g_{11}(V_{a1}sin\theta_{a1}-V_{a2}sin\theta_{a2})+b_{11}(V_{a1}cos\theta_{a1}-V_{a2}cos\theta_{a2})+\\
&g_{12}(V_{b1}sin\theta_{b1}-V_{b2}sin\theta_{b2})+b_{12}(V_{b1}cos\theta_{b1}-V_{b2}cos\theta_{b2})+\\
&g_{13}(V_{c1}sin\theta_{c1}-V_{c2}sin\theta_{c2})+b_{13}(V_{c1}cos\theta_{c1}-V_{c2}cos\theta_{c2}). \quad (5)
\end{aligned}
$$

Similar equations can be derived for the other phases. Deriving the Jacobain function is straightforward. For example, the partial derivatives of the real part of Phase A current given by (4) with respect to the voltage magnitude and phase angle of Phase B voltage at the receiving end are given by:

$$\frac{\partial I_{a,real}}{\partial V_{b2}} = -g_{12}cos\theta_{b2} + b_{12}sin\theta_{b2} \quad (6)$$

$$\frac{\partial I_{a,real}}{\partial \theta_{b2}} = g_{12}V_{b2}sin\theta_{b2} + b_{12}V_{b2}cos\theta_{b2}. \quad (7)$$

The other partial derivatives can be derived in a similar way. The rest of the process is similar to [15].

B. Ensemble Kalman Filter-based State Estimation

We extend the EnKF-based state estimation process proposed in [12] to unbalanced three-phase systems and include the three-phase branch current measurements obtained from D-PMUs in the PMU data assimilation step. The basic idea of the EnKF-based method is to utilize the additional information provided by the load evolution model and the previous system state to improve the the accuracy of the estimator. The EnKF-based state estimation process is shown in Figure 2; it comprises a number of steps discussed in the following.

1) Initial Ensemble: The initial ensemble $X^0 = [x_1^0, x_2^0, ..., x_{ES}^0]$ is formed by adding perturbation to the pseudo-measurements. Here ES is the ensemble size which is chosen to be equal to 500 in this work, similar to [12]. Note that in this implementation, real and reactive power consumption of nodes in the primary network are considered as the states of the system. Thus, the state vector is represented by $x = [P_1, P_2, ..., P_N, Q_1, Q_2, ..., Q_N]$. These states can be easily converted to conventional phase angle and magnitude of nodal voltages by performing a load flow. The added perturbations represent the error statistics of the pseudo-measurements.

2) Ensemble Integration: In this step, which is essentially the prediction step of Kalman filter, the ensembles are individually updated based on the load evolution model as follows:

$$X_P^t = X^{t-1} + W \quad (8)$$

where $W = [w_1, w_2, ..., w_{ES}]$ and w_i is a vector of size $2N$ representing the uncertainty of the load evolution model.

3) Assimilation of Pseudo-Measurements: In this step, the pseudo-measurements are used to update the predicted states X_P^t. First, the time-correlated error is removed and then the pseudo-measurement error and model noise covariance matrices are utilized to calculate the Kalman gain matrix K. The updated ensemble X_U^t is calculated subsequently as discussed in [12].

4) Assimilation of Phasor Measurements: The measurements coming from D-PMUs are now utilized to update the X_U^t calculated in the previous step. The process is similar to [12], the only difference being that after assimilating the voltage phasors, the process is repeated again this time using the current phasors. First, an ensemble $Z_V = [z_1^V, z_2^V, ..., z_{ES}^V]$ is computed using the voltage measurements from D-PMUs by adding a perturbation matrix E_V drawn from a distribution which represents the D-PMU measurement error. Similar to WLS, each measurement vector z_i^V is related to the state vector by a function h, which is the power-flow solution in this case. In other words, to get the measurement function values for each member of the ensemble X_U^t, power flow analysis has to be performed. As the ensemble size is typically chosen between 500 and 1000 [16], solving power flow for each member makes the computational cost of running EnKF-based state estimation much higher than WLS.

To perform the assimilation for voltage phasors, an augmented ensemble $\hat{X}_U^t$ is formed as follows:

$$\hat{X}_U^t = [\hat{x}_1, \hat{x}_2, ..., \hat{x}_{ES}] \quad (9)$$

where $\hat{x}_i = [x_i^T, h^T(x_i)]$. Now the updated ensemble X_V^t can be calculated by:

$$X_V^t = X_U^t + K_V(Z_V - \hat{H}\hat{X}_U^t) \quad (10)$$

$$K_V = \text{cov}(X_U^t, \hat{H}\hat{X}_U^t)\left(\text{cov}(\hat{H}\hat{X}_U^t) + \text{cov}(Z_V)\right)^{-1}. \quad (11)$$

where $\hat{H}$ is a selection matrix. After updating the ensemble using the D-PMU voltage measurements, the update process is repeated another time with X_U^t replaced by X_V^t for assimilating D-PMU current measurements. This part is different from [12]. In particular, an ensemble $Z_I = [z_1^I, z_2^I, ..., z_{ES}^I]$ is computed similar to Z_V, and then an augmented ensemble is formed as:

$$\hat{X}_V^t = [\hat{x}_1, \hat{x}_2, ..., \hat{x}_{ES}] \quad (12)$$

where $\hat{x}_i = [x_i^T, h^T(x_i)]$. Now the updated ensemble X_I^t can be calculated by:

$$X_I^t = X_V^t + K_I(Z_V - \hat{H}\hat{X}_V^t) \quad (13)$$

$$K_I = \text{cov}(X_V^t, \hat{H}\hat{X}_V^t)\left(\text{cov}(\hat{H}\hat{X}_V^t) + \text{cov}(Z_I)\right)^{-1} \quad (14)$$

Finally, the average of the calculated ensemble at time t, $X^t = X_I^t$, will give the estimated states. X^t is then used for ensemble integration in the next timestep. More information about the EnKF-based state estimator can be found in [12].

IV. Experimental Results

To evaluate the proposed state estimators, we use the 33-bus test system [17] as the primary distribution network. We also consider the secondary (low voltage) feeders in our simulations to get more accurate results. To model the secondary network, we adopt the IEEE European low voltage test feeder [18]. It is assumed that a low-voltage feeder is connected to each of the primary nodes. Figure 3 illustrates how the low voltage network is connected to one of these nodes, i.e., Node 25. Low-voltage networks with the same configuration are connected to all the nodes of the primary system.

There are 55 low-voltage single-phase loads under each primary node resulting in an unbalanced three-phase network. To represent the loads, we utilize sample household consumption data provided in the ADRES-CONCEPT project [19][2] The data set contains real and reactive power consumption of 30 households with 1-second resolution over two weeks: one week in winter and one in summer. Since our simulation is done for a 24-hour time window, the data is sliced into 24-hour segments. Therefore, in total 420 sample 24-hour load consumption data are obtained. We then add random Gaussian noise with 10% standard deviation to each sample to increase the size of data set; we specifically create a total of 4200 unique sample household load data. We further increase the original 1-second resolution of the load data to 500 milliseconds by using linear interpolation. This allows for studying how the delay in receiving D-PMU measurements could influence the state estimation accuracy.

We also use the real power consumption at the primary nodes provided in [17] to determine the appropriate level of aggregation at each low-voltage node (i.e., the houses connected to the same low-voltage node). We select houses randomly and connect them to each secondary node until the sum of all loads in the low-voltage network under each primary node reaches the load given in the 33-bus system data. It is assumed that all load nodes at the secondary distribution network are equipped with smart meters. Although these meters are capable of recording voltage magnitude in addition to active and reactive power, we only utilize the power data. We also assume that the smart meters report the data at the end of day. We utilize this data to estimate aggregated load demands at the primary nodes. The aggregated load demands are then used to forecast the day-ahead load demands (i.e. pseudo-measurements). As this forecasting is not within the scope of this study, we assume that such data is available for all primary nodes (per phase).

To get the required data for implementing WLS and EnKF, the loads connected to the low-voltage feeder of each primary node are aggregated to generate the primary load profiles (active and reactive power consumption at each primary node). The pseudo-measurements are then obtained by calculating the mean and standard deviation of the aggregated load profiles at each primary node for one-hour intervals. The load profiles are also used to calculate the load evolution model at each primary node for the whole simulation period (i.e. 24 hours). The error time-correlation for each interval is also calculated using the load profiles.

[2]The data was generated in the research project "ADRES-Concept" (EZ-IF: Developement of concepts for ADRES- Autonomous Decentralized Regenerative Energy Systems, project no. 815 674). This project was funded by the Austrian Climate and Energy Fund and performed under the program "ENERGIE DER ZUKUNFT".

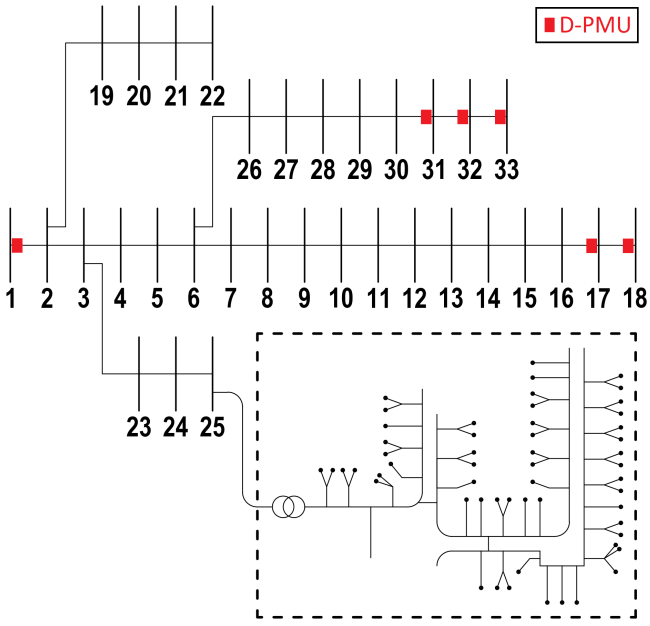

Fig. 3. The one-line diagram of the modified IEEE 33-bus test system. The IEEE European low-voltage system is connected to each of the nodes in the primary network.

We add a Gaussian white noise with 0.017% standard deviation to the voltage and current phasors obtained by solving power flow at each timestep to simulate D-PMU measurements. The standard deviation is chosen according to the specification of a commercial D-PMU device, dubbed as μPMU [20]. To evaluate the performance of the methods under different scenarios, the average root mean-squared error of voltage phasors [12] is used which is defined as:

$$\text{ARMSE} = \sqrt{\frac{1}{TN}\sum_{t=1}^{T}\sum_{i=1}^{N}(|V_i^{tr} - V_i^{es}|)^2} \qquad (15)$$

where V_i^{tr} and V_i^{es} are the true and estimated voltage phasor of node i, respectively.

For all test cases, unless mentioned otherwise, the time-step is 60 seconds, the delay is 500 ms, $\sigma_{PMU} = 0.00017$, and 5 D-PMUs are placed in the primary network. D-PMU locations are the same as [12] and are determined using a greedy method [21]. Specifically, the D-PMUs are placed in the network according to the following map:

$$\rho = \{33, 32, 31, 18, 17, 30, 16, 29, 15, 14, 13, 28, 12, 11, 10, 9, 8, 27, 26, 17\}$$

Note that 20 is the maximum number of D-PMUs considered in our work. For example, if we are to place 5 D-PMUs in the network, we connect them to nodes $33, 32, 31, 18, 17$, as shown in Figure 3. The substation is always equipped with a D-PMU. We assume that a D-PMU measures voltage and current phasors of all three phases.

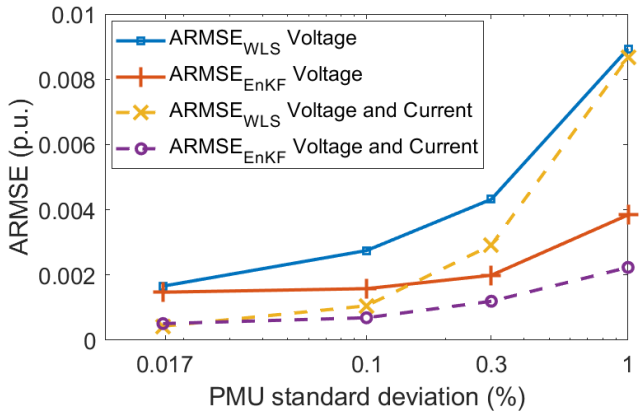

Fig. 4. ARMSE of WLS and EnKF for different PMU standard deviation values. Note that the x-axis is logarithmic.

Our code is written in MATLAB and the network is simulated in OPENDSS [22] which is responsible for calculating the nodal admittance matrix and solving power flow equations.

A. Effects of PMU's Accuracy

To show how the accuracy of D-PMU measurements can affect the accuracy of the results, we consider different standard deviations for D-PMU readings from 0.017%, which is the accuracy of μPMU [20], up to 1%. The PMU accuracy limit defined in IEEE Standard c37.118.1-2011 [23] is 1% which corresponds to 0.33% standard deviation. Figure 4 shows ARMSE values for WLS and EnKF, assuming that 5 D-PMUs are placed at the same nodes in each case.

It can be seen that for all cases having both voltage and current measurements from D-PMUs gives more accuracy compared to just considering voltage measurements. For 1% standard deviation, EnKF outperforms WLS in both cases: using just voltage measurements, and using both voltage and current measurements. The difference between EnKF and WLS becomes smaller as PMU measurements become more precise. For the highest precision considered in our study, which pertains to the existing D-PMU technology, WLS with voltage and current measurements gives the most accurate results. We attribute this to the fact that when the PMU measurement error is large, the load evolution model derived from historical data can be more important for reducing the estimation error, whereas when the measurement error is small, the accurate online measurements outcompete the historical data.

B. Effects of Delay

In many simulation studies, it is assumed that the PMU data is received instantaneously. However, in practice, there are always some delays associated with PMUs, including the processing and communication delay which is typically on the order of tens of milliseconds, and the buffering delay which could reach hundreds of milliseconds. Here, to investigate the effect of these delays on the performance of the state estimation methods, 500ms delay is considered. Similar to the previous cases, it is assumed that 5 D-PMUs are installed at the same nodes for all test cases. The ARMSE values of WLS and EnKF methods averaged over 5 independent runs are compared with or without delay in Table I. It can be seen that this delay does not have much impact on the performance of these methods, especially when only voltage measurements are available. This suggests that phasor measurements can be buffered at the D-PMU device and sent periodically to the utility data centre or other aggregation nodes to carry out state estimation, without sacrificing accuracy.

TABLE I
THE EFFECT OF DELAY ON THE ACCURACY OF THE METHODS

Method	No delay	500ms delay
WLS w/ voltage	0.001677	0.001685
EnKF w/ voltage	0.001471	0.001482
WLS w/ voltage and current	0.000426	0.000468
EnKF w/ voltage and current	0.000509	0.000544

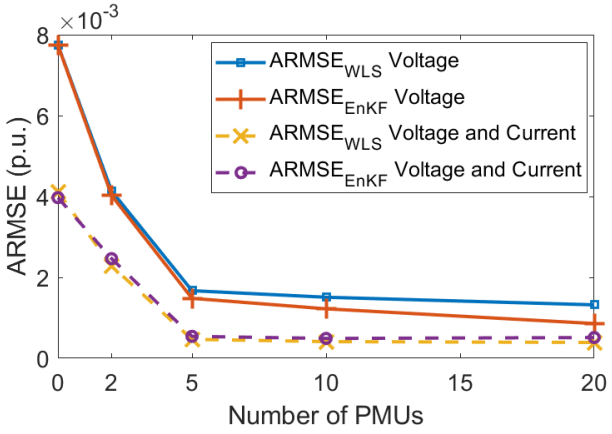

Fig. 5. ARMSE of WLS and EnKF for different number of PMUs.

C. Effects of the Number of D-PMUs

In this section we investigate whether increasing the number of D-PMUs installed in the primary distribution network reduces the state estimation error. In all cases, we assume that the substation is always equipped with a D-PMU and place 0, 2, 5, 10, and 20 D-PMUs in other nodes in the primary network following the map provided at the beginning of this section. Figure 5 indicates the performance of all methods improves as we increase the number of D-PMUs. However, there is not much improvement after adding 5 D-PMUs, which implies that 5 D-PMUs are enough to obtain satisfactory accuracy. Moreover, WLS with both current and voltage measurements has the highest accuracy among the methods we considered.

D. Effects of the state estimation time step

To study the effect of state estimation time step on the accuracy of the methods, different values (from 20 seconds up to 10 minutes) are considered and the average results of 5 independent runs are shown in Figure 6. For all these cases, we consider 5 D-PMUs (as shown in Figure 3) with 500ms delay. It can be seen that when only voltage phasor measurements are considered, EnKF outperforms WLS for all time-steps, whereas when both voltage and current phasor measurements are considered, WLS outperforms EnKF.

V. DISCUSSION & CONCLUDING REMARKS

We carried out a thorough comparison between WLS and EnKF state estimation methods in the context of a distribution

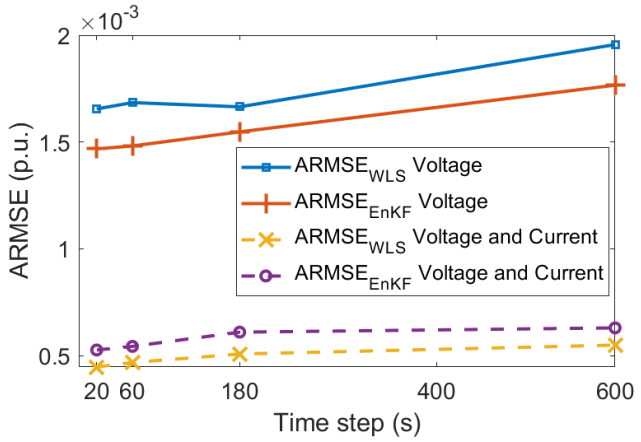

Fig. 6. ARMSE of WLS and EnKF-based state estimators for a different number of D-PMUs.

system, while taking into account practical considerations such as measurement error, data availability, and delay. We extended two state-of-the-art methods for real-time state estimation in unbalanced three-phase networks. Since the existing synchrophasor technology is capable of measuring current phasors in addition to voltage phasors, we leveraged current measurements to perform state estimation. Simulations conducted on a 33-bus test distribution system as the primary network and the IEEE European low-voltage test feeder as the secondary distribution system connected to each primary node, indicate that including current measurements can reduce the average RMS error of the methods by roughly $60 - 70\%$. A further comparison between WLS and EnKF methods, using current and voltage measurements, reveals that WLS is more accurate when the standard deviation of PMU error is 0.017%, which is the case for some of the currently available commercial D-PMUs, such as μPMU. Our experimental results also suggest that considering 500ms delay would not have a major impact on the accuracy of state estimation, especially when only voltage measurements are considered. Should the end-to-end delay increase beyond this level, the error will increase eventually. Another interesting finding is that installing only a small number of D-PMUs could significantly improve the accuracy of the methods. The average RMS error decreases quickly for the first 5 D-PMUs, but remains fairly constant afterwards. Finally, our simulations show that the state estimation time step does not have a major impact on its accuracy, especially when both voltage and current phasors measurements are incorporated. We observed that the accuracy of the methods does not change significantly when the time step is increased from 20 seconds to 10 minutes.

In future work, we plan to extend the methods by including some distributed generation units in the test system to study how these methods could handle the extra uncertainty introduced by them. We also intend to address the problem of PMU placement as some simple experiments revealed that it has a noticeable impact on the performance of both methods. Furthermore, we will strive to determine the minimum number of PMUs necessary to reach a desired level of accuracy.

Acknowledgment

We acknowledge the support of the Natural Sciences and Engineering Research Council of Canada (NSERC), [funding reference number RGPIN-2019-04349]. As a part of the University of Alberta's Future Energy Systems research initiative, this research was made possible in part thanks to funding from the Canada First Research Excellence Fund.

References

[1] A. P. Pegoraro *et al.*, "Bayesian approach for distribution system state estimation with non-gaussian uncertainty models," *IEEE Transactions on Instrumentation and Measurement*, vol. 66, no. 11, pp. 2957–2966, 2017.
[2] D. D. Giustina, A. P. Pegoraro, F. Ponci, and S. Sulis, "Electrical distribution system state estimation: measurement issues and challenges," *IEEE Instrumentation and Measurement Magazine*, vol. 17, no. 6, pp. 36–42, 2014.
[3] G. T. Heydt, "The next generation of power distribution systems," *IEEE Transactions on Smart Grid*, vol. 1, no. 3, pp. 225–235, 2010.
[4] A. Monticelli, *State Estimation in Electric Power Systems*. Springer, 1999.
[5] C. Muscas *et al.*, "Multiarea distribution system state estimation," *IEEE Transactions on Instrumentation and Measurement*, vol. 64, no. 5, pp. 1140–1148, 2015.
[6] M. E. Baran and A. W. Kelley, "State estimation for real time monitoring of distribution system," *IEEE Transactions on Power Systems*, vol. 9, no. 3, pp. 1601–1609, 1994.
[7] M. Pau, P. A. Pegoraro, and S. Sulis, "Efficient branch-current-based distribution system state estimation including synchronized measurements," *IEEE Transactions on Instrumentation and Measurement*, vol. 62, no. 9, pp. 2419–2429, 2013.
[8] A. Primadianto and C. Lu, "A review on distribution system state estimation," *IEEE Transactions on Power Systems*, vol. 32, no. 5, pp. 3875–3883, 2017.
[9] B. C. Singh, R. Pal and R. A. Jabr, "Choice of estimator for distribution system state estimation," *IET Generation, Transmission and Distribution*, vol. 3, no. 7, pp. 666–678, 2009.
[10] S. C. Huang, C. N. Lu, and Y. L. Lo, "Evaluation of ami and scada data synergy for distribution feeder modeling," *IEEE Transactions on smart Grid*, vol. 6, no. 4, pp. 1639–1647, 2015.
[11] S. Sarri *et al.*, "State estimation of active distribution networks: Comparison between WLS and iterated kalman-filter algorithm integrating PMUs," in *PES Innovative Smart Grid Technologies Europe*. IEEE, 2012.
[12] C. Carquex, C. Rosenberg, and K. Bhattacharya, "State estimation in power distribution systems based on ensemble kalman filtering," *IEEE Transactions on Power Systems*, vol. 33, no. 6, pp. 6600–6610, 2018.
[13] M. Pau, P. A. Pegoraro, and S. Sulis, "Performance of three-phase wls distribution system state estimation approaches," in *International Workshop Appl. Meas. Power Syst.* IEEE, 2015.
[14] O. Ardakanian *et al.*, "On identification of distribution grids," *IEEE Transactions on Control of Network Systems*, 2019.
[15] A. Abur and A. G. Exposito, *Power System State Estimation: Theory and Implementation*. CRC Press, 2004.
[16] G. Evensen, "The ensemble kalman filter: theoretical formulation and practical implementation," *Ocean Dynamics*, vol. 53, 2003.
[17] M. E. Baran and F. F. Wu, "Network reconfiguration in distribution systems for loss reduction and load balancing," *IEEE Transactions on Power Delivery*, vol. 4, no. 2, pp. 1401–1407, 1989.
[18] IEEE PES distribution systems analysis subcommittee, radial test feeders. [Online]. Available: http://sites.ieee.org/pes-testfeeders/resources/
[19] ADRES dataset. https://www.ea.tuwien.ac.at//projects/adres_concept/EN/. [Online].
[20] PSL, "MicroPMU Data Sheet," https://www.powerstandards.com/downl-oad/micropmu-data-sheet/, [Online].
[21] S. Schenato *et al.*, "Bayesian linear state estimation using smart meters and pmus measurements in distribution grids," in *SmartGridComm*. IEEE, 2014.
[22] R. C. Dugan, "Reference guide: The open distribution system simulator (OpenDSS)," *Electric Power Research Institute, Inc*, vol. 7, 2012.
[23] "IEEE C37.118.1-2011 - IEEE Standard for Synchrophasor Measurements for Power Systems," 2011.